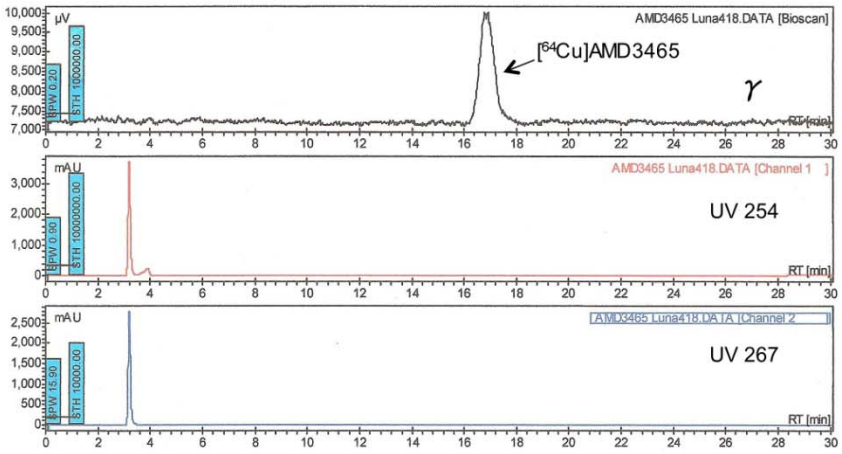

Supplemental Figure 1. HPLC chromatogram of [^{64}Cu]AMD3465.

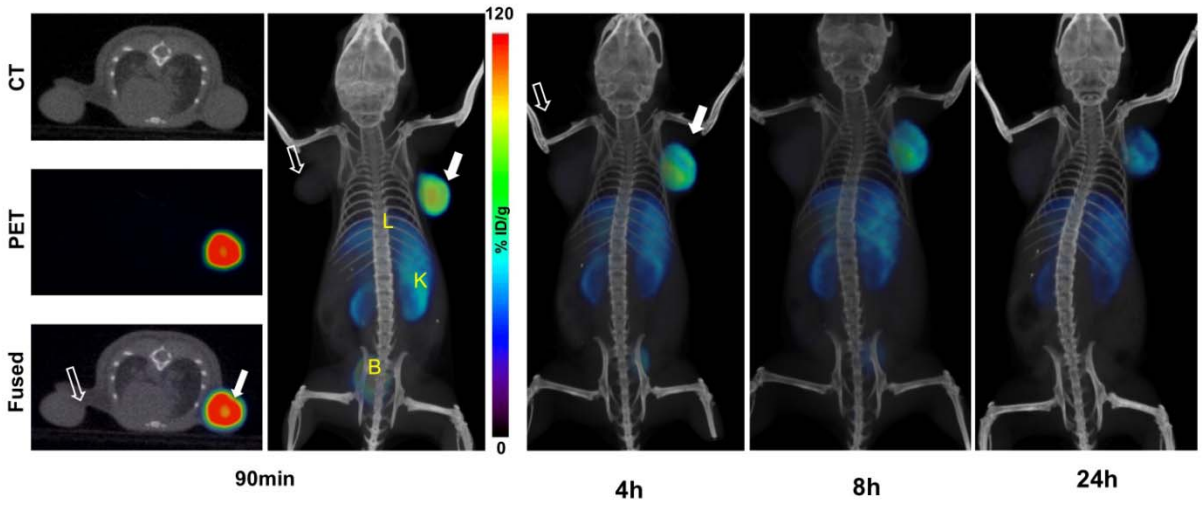

Supplemental Figure 2. PET/CT imaging of CXCR4 expression in subcutaneous brain tumor xenografts with [^{64}Cu]AMD3465. NOD/SCID mice bearing U87 and U87-stb-CXCR4 glioblastoma xenografts on the left and right flanks, respectively, were given approximately 9.25 MBq (250 μCi) of ^{64}Cu-labeled radiotracers *via* tail vein injection and PET/CT images were acquired. **A**, representative transaxial PET, CT and fused sections of both the tumors from a [^{64}Cu]AMD3465 injected mouse at 90 min post-injection; **B**, volume rendered whole body images of [^{64}Cu]AMD3465 at 90 min, 4h and 8h and 24 h post injection. All images were decay corrected and scaled to the same maximum threshold value. Unfilled arrow, U87 tumor; solid arrow, U87-stb-CXCR4 tumor; L, liver; K, kidney; B, bladder.

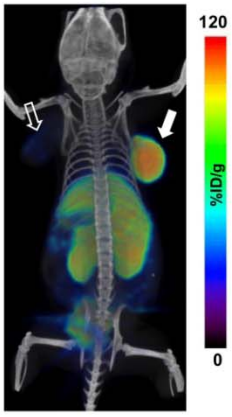

Supplemental Figure 3. PET/CT imaging of CXCR4 expression in subcutaneous brain tumor xenografts with [^{64}Cu]AMD3465. NOD/SCID mice bearing U87 and U87-stb-CXCR4 glioblastoma xenografts on the left and right flanks, respectively, were given approximately 9.25 MBq (250 μCi) of ^{64}Cu-labeled radiotracers *via* tail vein injection and PET/CT images were acquired. Volume rendered whole body image of [^{64}Cu]AMD3465 at 90 min post injection on a low %ID/g scale. Unfilled arrow, U87 tumor; solid arrow, U87-stb-CXCR4 tumor; L, liver; K, kidney; B, bladder.